The Climate Report

Vol. 3, No. 3, Summer 2002

In This Issue

Letter from the Editor

Over the past two decades, the scientific community has discovered a number of large-scale ocean-atmospheric phenomena, which have been shown to be the leading drivers of year-to-year climate variability in many regions around the world. Examples of these phenomena are the El Niño-Southern Oscillation (ENSO), the Arctic Oscillation (AO) and its regional manifestation the North Atlantic Oscillation (NAO), the Northern Pacific Decadal Oscillation (PDO). The ability to forecast these phenomena with useful lead-times will lead to significant improvements in the skill of seasonal forecasts over the U.S. and many other regions worldwide.

In the first article, Dr. Gilbert Compo and his co-authors, who are among the leading scientists in studying the dynamics of ENSO and its impacts, present their results on the predictability of anomalous storm tracks during El Niño and La Niña years. In the second article, Dr. Balaji Rajagopalan and his co-authors, report the results of the Phase I of a NOAA-sponsored project, investigating the relationships between ENSO, NAO, and the Tropical North Atlantic (TNA) sea surface temperatures (SST) on "Named Storm" frequency and landfall in the Atlantic basin. In the last article, Dr. Daoyi Gong, an associate professor at the Beijing Normal University, discusses the impacts of AO on the East Asian climate.

Maryam Golnaraghi, Editor

Predictability of Anomalous Storm Tracks

By Gilbert P. Compo, Prashant D. Sardeshmukh, and Cecile Penland*

** Corresponding author*

Introduction

Given that El Niño/Southern Oscillation (ENSO) is arguably the largest predictable signal in the climate system on seasonal to interannual time scales, it is not surprising that numerous studies have been devoted to investigating its global impacts. Most of these have focused on seasonal mean changes, including the seasonal mean temperature and precipitation. An ENSO event can, however, also affect the statistics of weather within a season, and perhaps even an individual storm. These effects can be distinct from the effects on seasonal mean quantities, and can have important practical implications. For instance, one may imagine a situation in which El Niño alters the occurrence of both dry spells and wet periods in a winter. The effect is a meaningful change in the risk of extreme weather, even though little seasonal mean signal is evident.

Extreme weather is largely associated with day-to-day variations of storm activity. Since the 1800's, surface low pressure systems have been tracked on maps, and it has been noticed that they follow preferred paths, known as "storm tracks." In the 1970's, researchers found that the variance of fluctuations in the mid-troposphere (500 mb height) on a time scale of less than a week demarcated these storm tracks in the Pacific and Atlantic regions. Following these variations in the vertical motions of the mid-troposphere (500-mb) represents a useful way of measuring the storm tracks.

After the discovery of the storm tracks, researchers observed that they varied from year-to-year, and have linked their interannual variation, in part, to ENSO. Seasonal mean precipitation, which is related to vertical motion in the atmosphere, also has interannual variations that are associated with ENSO. In this study we ask, how predictable are the ENSO effects on the storm tracks and seasonal mean precipitation? Are they related? And, what is the associated effect on the risk of extreme precipitation?

Measuring predictability

Usually, predictability is assessed for seasonal mean quantities, but it can equally be measured for the statistics of weather within a season. To assess the predictability, assume that a forecast system generates several possibilities, an ensemble, and issues the ensemble mean as the forecast. The variance of this ensemble is the uncertainty or "noise" in the forecast. If we evaluate the skill of the forecast using a correlation, ρ, between the forecasted mean, "the signal" and what actually happens, then the expected skill is known from analytical expressions and shown in Figure 1. The signal-to-noise ratio, $\boldsymbol{\mathcal{S}}$, is the ratio of the forecasted mean to the forecasted spread or standard deviation. For the same $\boldsymbol{\mathcal{S}}$, the skill increases as the number of possibilities, the ensemble size used to make the forecast, varies from 1 to infinity. These predictability curves are independent of the distribution that is being predicted. It could be bell-shaped or not, and the relationship between $\boldsymbol{\mathcal{S}}$ and ρ still holds. The curve for an infinite ensemble, ρ_∞, represents a hard predictability limit with a perfect model. It shows that to produce "useful" forecasts with anomaly correlations greater than 0.6, $\boldsymbol{\mathcal{S}}$ needs to be greater than 0.75. To produce "excellent" forecasts, with anomaly correlations greater than 0.9, $\boldsymbol{\mathcal{S}}$ must be greater than 2.

Figure 1: (a) Theoretical predictability curves for ensemble sizes of 1, 5, 25, and infinity as a function of the signal-to-noise ratio, S. The solid vertical bar indicates the maximum distance (-0.25) between ρ_1 and ρ_∞ curves obtained at $S=1/\sqrt{3}$. (b) The ρ_1 and ρ_∞ are copied from the upper panel. The dashed curves show the modified predictability ρ_∞ with a non-zero systematic error whose magnitude S_ε is 50% and 150% that of S. [From Sardeshmukh et. al., 2000.]

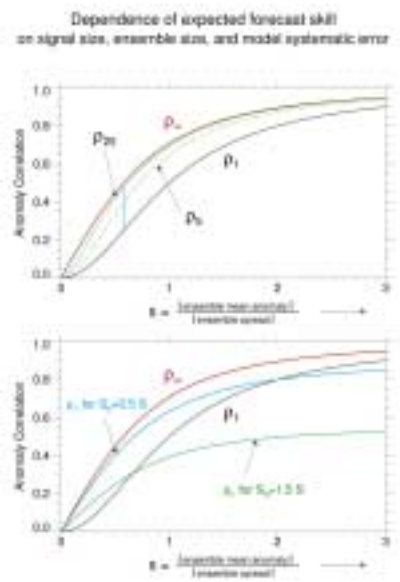

The curves in Figure 1 also show the advantage of using several ensemble members to make a forecast. Using a 25-member ensemble, ρ_{25} shows that the expected skill is nearly that of an infinite member ensemble. Unfortunately, to determine $\boldsymbol{\mathcal{S}}$ accurately (say within ±30%) more than 45 members are needed.

Forecasting the storm tracks

How might we make a forecast of the storm track for an individual season? One might think of approaching the problem empirically, using observations of the past 50+ winters. For example, one might fit a linear regression model of the storm tracks over the past 50 years to an index of ENSO such as central equatorial Pacific sea surface temperatures in the Niño3.4 region (5°S-5°N and 120°W-170°W). For an individual season, using a forecast of Niño3.4, the linear regression model predicts the expected storm track strength and pattern. The noise in this forecast might be the standard error of the regression fit. This approach would assume that,

i. The storm track response to ENSO is linear,

ii. ENSO does not affect the noise of the storm track,

iii. All the relevant probability distributions involved are Gaussian.

A natural alternative is to approach the problem with a dynamical numerical model. It is reasonable to expect general circulation models (GCMs), with their comprehensive nonlinear dynamics and also with many more variables in space and time than can be treated adequately in the observational record, to perform much better than empirical models. Nonetheless, two factors work against the fulfillment of such expectations. First, in a chaotic atmosphere a single run of GCM is only meaningful for two weeks at most. This chaos is associated with unpredictable nonlinear interactions in the atmosphere. The problem of predicting seasonal statistics becomes a probabilistic one, where the best one can do is use the same sea surface temperatures as a boundary condition and form an ensemble of possible climate outcomes by running the GCM many times from different atmospheric starting points ("initial conditions"). The mean of this ensemble becomes the expected value and is issued as the forecast. The spread of this ensemble is the uncertainty in the forecast. These two quantities, the forecast mean and spread, when the GCM ensemble has 100 or more members, allow us to estimate the ***S*** in Figure 1, with some confidence.

To the extent that the nonlinear interactions are unpredictable, or can be represented as linear plus noise, the GCM advantage over empirical methods is lost. To have an advantage, a GCM must show nonlinear effects in the ensemble mean and spread of the response to ENSO conditions. The recent work of Sardeshmukh et al. (2000) shows that a GCM can have a nonlinear response to ENSO in both the mean and the spread.

Second, the systematic error of a GCM may be substantial enough that the skill is much lower than expected for a perfect model. This is shown in the lower panel of Figure 1 for systematic errors that are 50% larger and 50% smaller than the signal itself. The flattening of the predictability curve when systematic error is included may help explain why many different GCMs have similar skill predicting the observed seasonal mean atmospheric circulation, but have widely divergent estimates of the signal-to-noise ratio.

Empirical and GCM predicted storm track signals for El Niño and La Niña

With these considerations in mind, we have estimated, using past observations, the storm track anomalies associated with ENSO for a particular set of winter [January through March, JFM] events: El Niño winter of 1987, and La Niña winter of 1989 given the historical El Niño and La Niña composite storm tracks. The composites were derived from the storm tracks averaged separately over the 11 strongest El Niño events and 11 strongest La Niña events in the historical record from 1948-2000. El Niño and La Niña are determined from the JFM average of the equatorial Pacific sea surface temperature anomaly in the Niño3.4 area. The storm track averages were subtracted from the storm track average during the 17 most neutral ENSO years to form the El Niño and La Niña storm track anomalies. The observational prediction for the 1987 El Niño storm track is then the historical El Niño composite scaled by the magnitude of the 1987 Niño3.4 index relative to all El Niños. The 1989 La Niña storm track prediction is formed similarly. This provides us with an observational estimate of the storm track "signal" for 1987 and 1989. These storm track anomalies for El Niño and La Niña are shown in the upper panels of Figure 2. Anomalies that are larger than expected by chance are shaded, with increased storm activity indicated in blue, and decreased storm activity indicated in yellow.

We then ask, how different are the signals the National Centers for Environmental Predictions (NCEP) atmospheric GCM predicts using the observed global sea surface temperature in JFM 1987 and JFM 1989? To make the GCM prediction, we run the model from 180 different atmospheric starting points ("initial conditions") but using the same sea surface temperatures each time. Using these 180 initial conditions, we have made predictions for 1987 El Niño, for 1989 La Niña, and for

climatological sea surface temperatures (our analogue to the neutral ENSO average). Of these runs, we have 60 for El Niño, 60 for La Niña, and 90 for climatological SSTs available at daily resolution for our storm track analysis, and 180 each for El Niño, La Niña, and climatological seasonal mean JFM precipitation. This 540-member ensemble is the largest used to date for this type of analysis.

Figure 2: The storm track anomalies for the 1987 El Niño and 1989 La Niña predicted from observations and GCM experiment. The storm tracks are represented by 500-mb vertical velocity fluctuations with periods between 2 and 7 days. Statistically significant increased (decreased) storm activity is shaded blue (yellow). The contour interval is 0.02 Pa/sec.

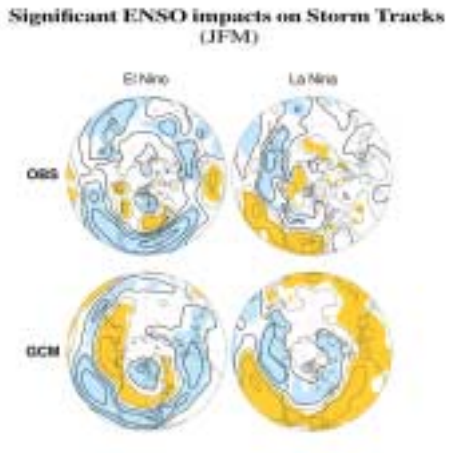

The GCM predicted storm track anomalies are shown in the lower panels of Figure 2. The comparison of the GCM prediction and observational prediction is not clean, in that the observational panels have used the average over several events, each with different sea surface temperatures, while the GCM predictions takes into account only the details of the individual 1987 El Niño and 1989 La Niña sea surface temperatures. Despite these differences, in both the GCM and observational predictions, several of the gross features of the ENSO effect on storm tracks are seen, including shifted storm tracks over North America, with El Niño having more storm activity along the southern US and La Niña reduced storm activity in the southern US. The similarity then, is reassuring, in that this GCM is suitable for studying the ENSO effect on storm tracks and that El Niño and La Niña differences found in the large GCM sample may be realistic and meaningful.

Several new features of the ENSO effect on storm tracks are evident in Figure 2 that are significant both because of the large number of samples and their mutual consistency. For example, during El Niño, a belt of increased storm activity extends from South Asia, across the Pacific, North America, the Atlantic, and into Eurasia. A region of decreased storminess lies to the north. While consistent with previous regional studies, this coherent hemispheric response has not been previously observed.

In the North Atlantic sector, the observational and GCM predicted signals for La Niña differ. The result suggests that this region may have significant storm track changes from ENSO event to event or, of course, that model error may be large there.

Predictable storm track anomalies

Given the relatively good comparison between the observational and GCM predicted signals for the 1987 El Niño and 1989 La Niña, the question remains as to the practical value of these signals. This can be assessed using the signal-to-noise ratio and the expected anomaly correlation from Figure 1. While the observational sample is too small to accurately estimate the signal-to-noise ratio, we have a sufficient sample from the GCM.

The largest storm track anomalies, in terms of the signal-to-noise ratio, are plotted in the top panels of Figure 3. The red and yellow colors indicate where storm activity is decreased; the blues indicate where storm activity is increased. The contour interval is 0.25 with the 0 contour suppressed. The darkest reds and blues show where a useful forecast, with an anomaly correlation greater than 0.6, can be expected. These regions are limited to the eastern Pacific and western North America. Around the remainder of the hemisphere, for both El Niño and La Niña, signal-to-noise ratio magnitudes for storm track anomalies range from 0.25 to 0.5, which corresponds to expected correlations between 0.24 and 0.44. For some applications, expected skill of this magnitude may still be of value to decision makers.

Our interest here is not in the storm track anomalies alone, but how they relate to the predictable seasonal mean precipitation. The signal-to-noise ratios for GCM predicted JFM precipitation anomalies for the 1987 El Niño and 1989 La Niña are shown in Figure 3. The strongly predictable precipitation signals correspond well with the predictable storm track regions. Over the hemisphere the patterns also agree well. Over the central US during El Niño, no significant precipitation signal is seen despite the significant storm track anomalies. Our research suggests that this may be a region where sensitive cancellations can occur between storm track anomalies and the seasonal mean flow. Because the storm track variations are only weakly governed by the seasonal mean flow, these relations between the daily weather statistics and the seasonal precipitation suggest that improved prediction of seasonal mean precipitation will require improved

representation of storm activity in global models. It also suggests that empirical prediction methods of seasonal mean precipitation may be improved by including storm track variations.

In regions where the seasonal mean precipitation anomaly is not highly predictable, but still has a significant signal, does useful information remain? The altered risk of extreme anomalies is one such piece of information that may be of value to a wide-range of decision makers. The four lower panels of Figure 3 show the altered risk of extreme seasonal mean precipitation for El Niño and La Niña. Several regions where the risk has changed by more than 100% are evident in the darkest red and blue shading. The original risk of wet conditions is defined as the probability of exceeding the climatological local mean plus one standard deviation. The altered risk is the difference between the original risk and the risk under El Niño or La Niña conditions. We divide the altered risk by the original risk to get percent changes in risk, and this is plotted in the lower panels of Figure 3. The contour interval in Figure 3 begins at a 50% change in risk, with contours every 25% thereafter. Given our large sample size, altered risks of 50% or more are significantly greater than what one would expect by chance. For extreme wet conditions, blue shading denotes increased risk of wet, and reds denote decreased risk of wet. For extreme dry conditions, increased risk of dry is denoted by red and decreased risk of dry is denoted by blue. The darkest reds and blues correspond to a 100% change in the risk. Note that decreases in risk cannot be less than 100%.

The altered risks in Figure 3 correspond well with the significant signals seen in the seasonal mean precipitation panels. Some regions show substantial differences in the magnitude of the altered risk. For instance, over Florida, El Niño doubles the risk of wet conditions while only halving the risk of dry. The altered risk can also be in the same direction for both El Niño and La Niña. Over western Africa, both show a decreased risk of dry conditions, while El Niño also shows a decreased risk of wet conditions. Similarly, over the Middle East, both El Niño and La Niña show an increased risk of dry conditions. Such nonlinear changes are difficult to detect using empirical methods given the small sample size of the observational record.

Summary and conclusions

We have demonstrated that a large ensemble of atmospheric general circulation model runs can be used to estimate the predictable signals associated with El Niño and La Niña. Some of those signals may be nonlinear and difficult to detect with empirical methods that must rely on the small sample size of the historical record. The number of GCM runs needed to estimate predictability is much larger than is currently being used for similar studies; 100 or more GCM runs are needed for each ENSO event, rather than the 8-30 usually made.

Because of the relatively small signal to noise ratio, S, the expected predictability of the seasonal mean storm track and precipitation is relatively small, except in a few areas over the Pacific and western Atlantic. Accurate determination of S is still important, and may be dependent on the details of the individual ENSO event, so a large number of samples is needed. The advantages of an accurate determination of S may seem moot. It is not. For a large S, say greater than 3, only a few ensemble members are needed to make an excellent forecast. For a small S, say less than 0.5, the large number of ensembles still does not make a forecast with useful skill. However, for the intermediate values, the advantage of a large ensemble is useful for making a better forecast and for estimating the expected skill of that forecast. Figure 1b, though, reminds us that the systematic error in a forecasting system can completely eliminate this gain in forecast skill.

The ρ_∞ curve in Figure 1 strongly

Figure 3: (Upper four panels) The predictable storm track and seasonal mean precipitation anomalies for the 1987 El Niño and 1989 La Niña as measured by the signal-to-noise ratio *S*. from the GCM experiment Contour interval is 0.25 with the 0.0 contour suppressed. Positive (negative) values are shaded blue (red). (Lower four panels). Altered risk of extreme seasonal mean precipitation. Risks are shown relative to climatological risk. Contour interval is 25% beginning at 50%. Darkest colors show 100% change in risk. In the Wet risk panels, reds indicated decreased risk, blues indicate increased risk. In the Dry panels, reds indicate increased risk, blues indicate decreased risk. In all panels, blues correspond to wetter conditions, reds to drier conditions.

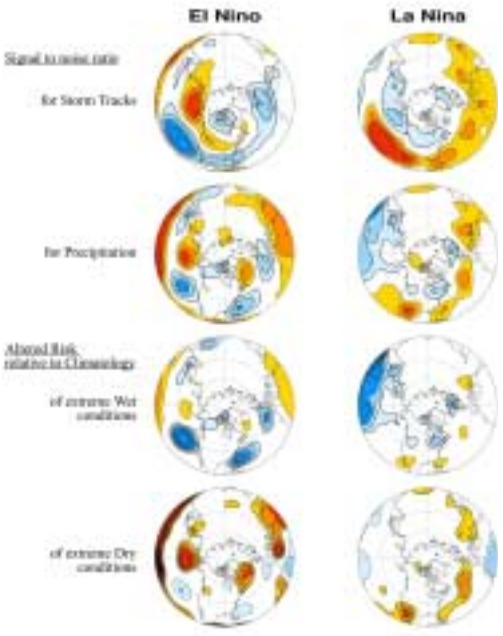

constrains the predictability of seasonal statistics during ENSO events, and because of this, even a perfect GCM's advantage over empirical forecasting methods may be small. The results here show, however, a GCM's ability to predict changes in the mean and the variability for an individual event give it a potentially huge advantage for predicting the altered extreme risk of seasonal mean precipitation and other quantities. The altered risk can be the same for El Niño and La Niña. Accurate estimates of these risks for future ENSO events will benefit not only from model improvements, but also from running large ensembles.

Suggested references and web sites

- The details of the study presented here can be found in:

Compo, G. P., P. D. Sardeshmukh, and C. Penland, 2001: Changes of Subseasonal Variability Associated With El Niño. *Journal of Climate*, **14**, 3356-3374.

Sardeshmukh, P. D., G. P. Compo, and C. Penland, 2000: Changes of Probability Associated with El Niño. *Journal of Climate*, **13**, 4268-4286.

- For a complete review of northern hemisphere storm tracks:

Hoskins, B. J. and K. I. Hodges, 2002: New perspectives on the Northern Hemisphere winter storm tracks. *Journal of Atmospheric Science*, **59**, 1041-1061.

- For ENSO impact on individual storms:

Barsugli, J.J., J.S. Whitaker, A.F. Loughe, P. D. Sardeshmukh, and Z. Toth, 1999: The Effect of the 1997/98 El Niño on Individual Large-Scale Weather Events. *Bulletin of the American Meteorological Society*, **80**, 1399-1411.

- For ENSO impact on precipitation and temperature extremes over the US:

Cayan, D. R., K. Raymond, and L. Riddle, 1999: ENSO and Hydrologic Extremes in the Western United States. *Journal of Climate*, **12**, 2881-2893.

Gershunov, A., and T. P. Barnett, 1998: ENSO Influence on Intraseasonal Extreme Rainfall and Temperature Frequencies in the Contiguous United States: Observations and Model Results. *Journal of Climate*, **11**, 1575-1586.

Smith, C. A. and P. D. Sardeshmukh, 2000: The Effect of ENSO on the Intraseasonal Variance of Surface Temperatures in Winter. *International Journal of Climatology*, **20**, 1543-1557.

- For the ENSO impact on European storms:

Fraedrich, K., 1994: An ENSO impact on Europe? A Review. *Tellus*, **46A**, 541-552.

- For the modern discovery of the storm track:

Blackmon, M.L., J. M. Wallace, N. C. Lau, and S. L. Mullen, 1977: An Observational Study of the Northern Hemisphere Wintertime Circulation. *Journal of Atmospheric Science*, **34**, 1040-1053.

** Dr. Gilbert P. Compo is a Research Scientist with the University of Colorado's Cooperative Institute for Research in the Environmental Sciences working at the NOAA-CIRES Climate Diagnostics Center. Active research areas include the global effects of ENSO on atmospheric probability distributions, the predictability of the effects of ENSO on storm tracks and blocking, data assimilation methods for historical observations, and time series analysis methods using wavelets. Dr. Compo holds a Ph. D. in Astrophysical, Planetary, and Atmospheric Sciences from the University of Colorado.*

Email: gpc@cdc.noaa.gov

Dr. Prashant D. Sardeshmukh is Associate Director of the NOAA-CIRES Climate Diagnostics Center and a Senior Research Scientist at the University of Colorado's Cooperative Institute for Research in the Environmental Sciences. His research areas include linear and nonlinear atmospheric dynamics with timescales from days to centuries, the atmospheric response to ENSO and the Madden-Julian Oscillation, fundamental stochastic dynamics, and the dynamics of ENSO. He has been a Joint Director of the National Center for Medium Range Weather Forecasts at New Delhi, India, and a Visiting Scientist at the European Center for Medium Range Weather Forecasting. Dr. Sardeshmukh holds a Ph. D. in Geophysical Fluid Dynamics from Princeton University.

Dr. Cecile Penland is a Physical Scientist with the National Oceanic and Atmospheric Administration at the NOAA-CIRES Climate Diagnostics Center. Her research areas include fundamental stochastic dynamics, linear inverse modeling, stochastic descriptions of geophysical systems, coupled modeling of atmosphere-ocean interaction, the dynamics of sea surface temperature variability in the tropical Oceans, and the global effects of ENSO. Dr. Penland holds a Ph. D. in Physics from the University of Texas at Austin.

Relationships Between Large Scale Climate Indices and Named Storm Frequency in the Atlantic Basin

By Balaji Rajagopalan, Yochanan Kushnir, Jennie Miller and Upmanu Lall*
**Corresponding author*

Introduction

Tropical and extra-tropical cyclones (hurricanes) lead to major natural disasters at sea and in the regions of landfall. These severe storms are characterized by intense precipitation and high winds. Named Storms (NS) include all tropical cyclones reaching a maximum sustained wind speed of at least 18 m/s (Neumann, et al. 1993). Their impact along the Atlantic Coast of North and Central America is often catastrophic to life, ecology, property, wetlands and coastal estuaries. The severity and frequency of major tropical storms is consequently of great interest for disaster planning and mitigation.

Over the years, investigators have identified large-scale climatic factors, such as the El Niño/Southern Oscillation (ENSO), Quasi Bi-ennial Oscillation (QBO)[1], Atlantic Sea Surface Temperatures (SSTs), and rainfall over Africa's Sahel region, that appear to affect the year-to-year variability in tropical cyclone activity (Gray, 1984a and Gray, 1990; Goldenberg and Shapiro 1996; Shapiro, 1982; Shapiro, 1989; Shapiro and Goldenberg, 1998; Bove et al., 1998). Recently, Elsner and Kocher (2000) found links between tropical cyclone activity and the preceding winter state of the North Atlantic Oscillation (NAO). Mechanistically, all these climatic phenomena are believed to regulate tropical storm formation via their effects upon upper tropospheric wind shear (Landsea, 1998). Events, which increase shear lead to a weaker hurricane season while events, which lower wind shear, make for an active season. These findings led to the development of statistical forecasting schemes for indicators of tropical cyclone activity during the stormy season (Gray 1984b; Gray et al., 1992,1993,1994; Hess et al., 1995).

The forecasting schemes by Gray and others typically predict the total number of named storms in a given year in the Atlantic basin. While these forecasts have been very useful, risks from hurricanes at a given coastal location are only indirectly reflected.

There are efforts underway to issue probabilistic forecast of landfalls at a few locations on the eastern coast of USA (Gray 1998; Gray et al., 2000). One step towards improving regional landfall forecasting is to examine the spatial variability of tropical named storm activity in the entire basin relative to various large-scale climate indicators.

This study explores the regional effects of climate indicators such as, ENSO, NAO and Tropical North Atlantic (TNA) SSTs, on named storm activity. A "bootstrap"[2] method is developed and used to analyze the spatial statistics of named storm incidence in the Atlantic basin, conditional on three large-scale climate indicators (ENSO, NAO, and TNA). In addition, a "t-test"[3] on the means of named storm incidence and other variables is also performed.

Data

The data sets used, cover the 112 years from 1886 to 1997. The data used can be described under three categories:

Storm data: The named storm data are obtained from the National Hurricane Center. This database contains information on named storms location, wind speed, and pressure for every six hours of the storm's existence. It includes all storms from 1886 to 1997. This dataset was modified (Mitchell, personal communication) to a daily time scale by selecting only the entries with the greatest of the four recorded wind speeds for each day.

Climate indicators: These consist of seasonal averages for winter (December-January-February-March: DJFM); spring (March-April-May: MAM) and summer (June-July-August: JJA)) of the following indices:

1) NIÑO3: Average, normalized equatorial Pacific SST anomalies

[1] QBO is a zonal wind index in the tropics. For more information see, http://tao.atmos.washington.edu/data_sets/qbo/.

[2] The bootstrap technique involves shuffling the data and randomly picking a data point (i.e., observation) year with replacement. Traditionally, the bootstrap has been used to estimate confidence limits on sample statistics like mean, standard deviation. Recent modifications to this technique have been applied to time series re-sampling and scenario generation.

[3] T-test is a statistical method to test the significance of difference in the means between two groups. The test can be performed assuming equal or unequal variances between the groups.

in the area 5°S-5°N and 150°W-90°W SST, obtained from the grid-point data of Kaplan et al. (1998).

2) TNA: Tropical North Atlantic SST index, normalized, area averaged SST anomaly in the region of 5°N-20°N, 20°W-40°W;

3) NAO index as defined by the difference in normalized SLP anomalies between Ponta Delgada (Azores) and Reykjavik (Iceland) (Hurrell, 1995).

Supplementary data: These data sets are obtained from NCEP/NCAR Re-analyses (Kalnay et al., 1996).

1) *U-Shear:* The difference in the U-component of the surface winds between 400mb and 850mb ($U_{400} - U_{850}$).

2) *V-steering winds:* The average of V-component of the surface winds between 600mb and 1000mb.

Methodology

We divide the Atlantic basin (20°W - 100°W; 5°N-45°N) into 5° x 5° boxes. The number of named storm days occurring in each box for each year is computed. The 112 years are divided into three categories based on the strength (High, Low, and Neutral) of a particular climate index in each season. "High" and "Low" boundaries are set at $\pm 0.75\sigma$, where σ is the standard deviation for each indicator. We use a "bootstrap" technique (Efron, 1991) to determine the grid boxes with significant differences in the median NS days relative to the three indicator categories. In other words, we seek to examine, for instance - is the median NS days at a grid box during "High" winter NAO significantly different from the median NS days at the same grid box during "Low" winter NAO, or Neutral winter NAO? Similarly, for other indicators and other seasons as well. Additionally, we use the t-test for differences in means between the categories (Helsel and Hirsch, 1992) to compare the results from the "bootstrap" method.

The bootstrap technique involves shuffling the data and randomly picking a year with replacement. Traditionally, the bootstrap has been used to estimate confidence limits on sample statistics like mean, standard deviation. Recent modifications to this technique have been applied to time series re-sampling and scenario generation (Lall and Sharma, 1996; Rajagopalan and Lall, 1999).

The dependence of the number of named storm days in each grid box on a climate index is assessed through a bootstrap procedure, designed to check for the significance of the median number of named storm days conditional on the "state" (e.g., high, neutral or low category) of the climate index of interest. The procedure used is outlined below:

1) For each climate index category I, identify the corresponding number of years n_i

2) Generate 1000 samples, each of length n_i by sampling with replacement from the original n_i years. Compute the median number of named storm days per year for each of the 1000 samples

3) Estimate the 5th, 50th, and 95th percentiles ($ns_{0.05,i}$, $ns_{0.5,i}$, $ns_{0.95,i}$) of the median number of named storm days per year from these 1000 estimates for the climate category.

4) Now compare the confidence limits of the medians across categories.

   a) Record a 0, for the comparison of categories i and j, if $ns_{0.05,j} \leq ns_{0.5,i} \leq ns_{0.95,j}$

   b) Record a 1, if $ns_{0.95,j} \leq ns_{0.5,i}$

   c) Record a 2, if $ns_{0.95,j} \leq ns_{0.05,i}$

In addition to the bootstrap technique we calculate the difference and perform a t-test (Helsel and Hirsch, 1992) on the averages of the variables that are of importance to tropical cyclone genesis and maintenance (e.g., U-Shear, V-steering winds, and SSTs) between the indicator categories. The t-test is performed at each grid box and the grid locations that show differences at 90% and 95% significance are colored. This will help identify regions in these fields where significant differences are shown in comparison to the differences in the NS days as seen in the bootstrap results and point at physical mechanisms associated with the anomaly in NS occurrence. Furthermore, we performed a t-test on the total number of storms generated in the basin, storms reaching the East coast of US and Florida, and storms reaching the Gulf coast, relative to different phases of the climate indices.

The above steps are repeated for all the climate indicators and for winter, spring and summer seasons, and the results are presented and discussed in the following sections.

Results

The spatial variation in the named storm days conditional to various climate indices is discussed. In each figure, only the significant boxes (with the significant criteria described in the previous section) are colored. Dark brown color indicates that the 95% confidence intervals of median number of storms during one phase of the climate indicator is

higher than the confidence limit of the comparing phase, dark purple color is used when the confidence interval is lower. Yellow color indicates that the 50th percentile of one phase of the climate indicator is greater than the 95% confidence intervals of the comparing phase, and light purple represents the opposite difference. The contours show the magnitude of difference in the mean NS days between the categories from the historical data. Because the data are rather noisy, we smoothed the difference using one pass of a two-dimensional binomial (1-2-1) filter. On the t-test figures dark brown and orange colors are for boxes with significant differences in the positive direction at 95% and 90% confidence levels, respectively and blue and purple, vice-versa. On all the figure captions the phase on the left is compared to the phase on the right (e.g., High - Low on the caption indicates that the High phase is compared to Low phase). This convention is followed in all the figures.

ENSO

Significant difference (reduction in the number of storms) in the NS days between the high and low categories of NIÑO3 during summer (Figure 1a), can be seen in the western half of the tropical Atlantic basin, west of 50°W. Relative to low phase of ENSO (La Niña) the high phases (El Niño) exhibits a substantial reduction (of up to 7 storm days per decade) in the NS activity. The differences are especially large along the coastal regions of U.S. This result corroborates with earlier findings that El Niño reduces storm activity in the Atlantic basin (Gray, 1984; Bove et al., 1999). Relative to the neutral phase, the high phase of ENSO also shows a reduced NS activity along the Florida coast, Gulf of Mexico and the Carribeans (Figure 1b). However, the significant boxes are much more scattered, unlike a coherent region in Figure 1a. The low phase does not show a clear and coherent signal relative to the neutral phase (Figure 1c).

Figure 1: Bootstrapped significant storm days for NIÑO3 (JJA) (a) between High phase and Low phase, (b) between High phase and Neutral phase, (c) between Low phase and Neutral phase. The contours are the difference in storm days between the categories that are compared per decade. (Dark brown color indicates that the 95% confidence interval of median number of storms during one phase of the climate indicator is higher than the confidence limit of the comparing phase, dark purple color is used when the confidence interval is lower. Yellow color indicates that the 50th percentile of one phase of the climate indicator is greater than the 95% confidence intervals of the comparing phase, and light purple represents the opposite difference).

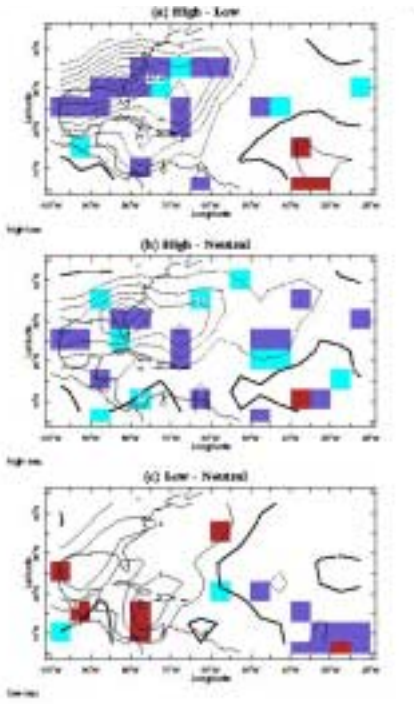

The differences in U-shear between the three phases of NIÑO3 during summer also reveal a consistent picture (Figure 2). Relative to the low phase, the high phase has significantly larger U-shear (Figure 2a) in the eastern tropical Pacific and western tropical Atlantic regions. The same is true relative to neutral phase (Figure 2b). It is known that large U-shear values inhibit the formation of tropical cyclones and their maintenance (Gray, 1984a; Goldenberg and Shapiro 1996). The opposite shear anomalies occur during low phases of ENSO (Figure 2c) but are not as spatially coherent. Consequently, high phase of ENSO corresponds to reduced NS storm activity and vice-versa. This can also be seen in the significant reduction in the number of storms in the entire basin, and in the landfall regions (see Tables 1 and 2).

Table 1: Total number of storms

Index	High	Neutral	Low
NAO (DJFM)	54.56	61.88	65.22
Niño (DJF)	60.14	62.88	57.54
Niño (JJA)	49.44	62.77	68.40
TNA (JJA)	81.90	58.72	43.07
TNA (MAM)	70.50	64.11	44.85

NAO

One of the surprising and interesting results of this study has been the significant difference in the storm activity associated with the state of NAO in the preceding winter. There is a general reduction (of up to 6 storm days per decade on the average) in NS activity over the western half of the tropical Atlantic basin (Figure 3a,b) following a winter of high NAO phase relative to low and neutral phases. Differences between low NAO phase and neutral are not coherent. A reduction in the V-steering winds in the western ocean region, during the summers following high NAO winters relative to low and neutral phases. The reduction in the V-steering is consistent with decreased NS activity. This also reflects in the reduction of landfall storms (Table 2) but not as much in the total number of storms generated in the entire basin (Table 2). Thus, it appears that winters with high NAO phase tend to create

conditions that steer storms away from the coast in the following summer.

The NAO also leaves a noticeable impact on summer SSTs in the tropical north Atlantic basin. After winters of high NAO phase SSTs are colder than normal from the coast of Africa to the Carribeans. This too tends to affect storm growth (see below). Overall the NAO effect opens way to predicting landfall over the US Atlantic coast.

TNA

Warmer temperatures in the TNA region, favors convection, less vertical wind shear and consequently aids in storm activity (Shapiro and Goldenberg, 1998). Consequently, enhanced NS activity can be seen over almost entire Atlantic basin between 15°N – 40°N, during high phase of TNA relative to low and neutral phases Interestingly, it is the negative phase of the index that is associated with high spatial coherence. This enhancement is significant even when the spring TNA values are used, which indicates a potential for predictability. We obtain similar results for summer TNA as well – which suggests that the spring SSTs in the TNA region persist quite a bit into the summer. The enhancement of NS activity can also be seen in Table 2, where a significant increase in the number of storms over the entire basin is seen, relative to a high phase of TNA.

Table 2: T-test results for total number of storms and landfalls

Index	High - Low	High - Neutral	Low - Neutral
T-Test Total Number of Storms			
NAO (DJFM)	12.8271	18.1664	69.3991
Niño (DJF)	61.3415	35.1560	23.0325
Niño (JJA)	1.0008	1.9510	78.7696
TNA (JJA)	99.9999	99.9605	0.2337
TNA (MAM)	99.9650	83.9695	0.1411
T-Test East Coast/Florida Landfall			
NAO (DJFM)	0.0841	0.5524	82.6282
Niño (DJF)	54.8535	40.6770	38.1861
Niño (JJA)	0.2906	0.3365	88.4558
TNA (JJA)	99.9045	99.1045	8.1474
TNA (MAM)	99.7894	94.7472	2.0640
T-Test Gulf Landfall			
NAO (DJFM)	1.6926	3.3525	75.6923
Niño (DJF)	48.4713	40.5604	43.3707
Niño (JJA)	1.5641	4.3859	84.3904
TNA (JJA)	99.9860	98.9792	0.9587
TNA (MAM)	99.7751	74.5128	0.3901

Figure 2: T-test based significant differences in the mean of U-shear for NIÑO3 (JJA) (a) between High phase and Low phase, (b) between High phase and Neutral phase, (c) between Low phase and Neutral phase. (Dark brown and orange colors are for boxes with significant differences in the positive direction at 95% and 90% confidence levels, respectively and blue and purple, vice-versa).

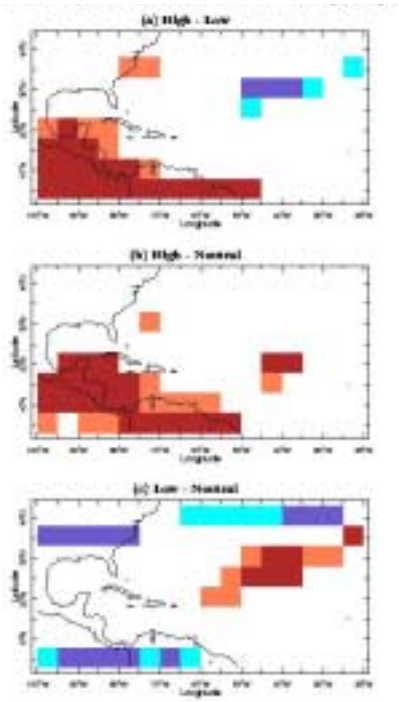

Discussion

Our results indicate that ENSO has an influence on the total number of storms generated in the basin, and also on the landfall storms. Furthermore, the high (or warm) phase of ENSO has a stronger impact than the low (or cold) phase. This corroborates earlier results (e.g., Gray, 1984a). Spring TNA also has an impact on the total number of storms and also on landfall storms. While, winter NAO seems to affect the landfall storms and not as much the total number of storms in the basin. The NAO predominantly is a mid-latitude phenomenon that has links to tropical and extra-tropical SSTs (Rajagopalan et al., 1998). This also underscores the relevance of mid-latitude climatic forcing to tropical cyclone activity (e.g., Elsner and Kocher, 2000). The results also suggest a strong potential for winter NAO and spring TNA in the probabilistic forecast of hurricanes, along with other predictors that have been identified so far.

We have demonstrated the utility of the bootstrap technique in visually identifying regions in the Atlantic basin that exhibit significant differences in NS activity and other variables that influence cyclone activity, relative to different phases of

Figure 3: Same as in Figure 1, but for NAO (DJFM). The colored regions have the same significance as in Figure 1.

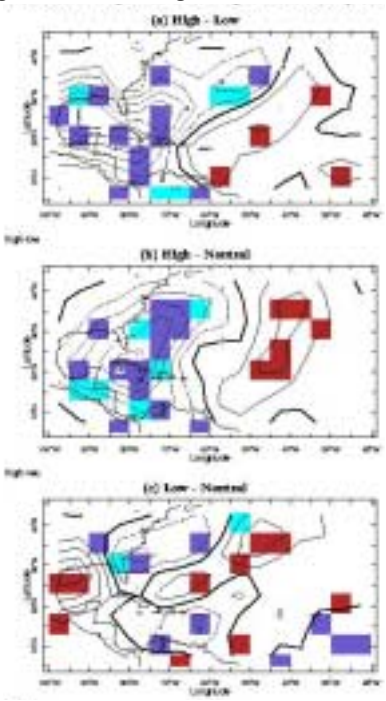

large-scale climate indicators. The method is easy to implement and handles non-Gaussian and non-linear structures in a natural way.

Acknowledgments

This work was supported by NOAA grant NA96GP0463. We thank Todd Mitchell of JISAO/U. Washington for providing the procedure for modifying 6-hourly storm track data to a daily time scale.

Suggested references and web sites

Bove, M.C., J. B. Elsner, C. W. Landsea, X. Niu and J. J. O'Brien, 1998: Effect of El Niño on U.S. Landfalling Hurricanes, Revisited. *Bulletin of American Meteorological Society*, **79**, 2477-2482.

Elsner, J. B., and B. Kocher, 2000: Global tropical cyclone activity: A link to the North Atlantic Oscillation. *Geophysical Research Letters*, **27**, 129-132.

Goldenberg, S.B. and L. J. Shapiro, 1996: Physical Mechanisms for the Association of El Niño and West African Rainfall with Major Atlantic Hurricane Activity. *Journal of Climate*, **9**, 1169-1187.

Gray, W.M. 1984a: Atlantic Seasonal Hurricane Frequency. Part I: El Niño and 30mb Quasi-Biennial Oscillation Influences. *Monthly Weather Review*, **112**, 1649-1668.

Gray, W.M. 1984b: Atlantic Seasonal Hurricane Frequency. Part II: Forecasting its Variability. *Monthly Weather Review*, **112**, 1669-1683.

Gray, W.M. 1990: Strong association between West African rainfall and US landfall of intense hurricanes. *Science*, **249**, 1251-1256.

Gray, W.M., C. W. Landsea, P. W. Mielke Jr., and K. B. Berry, 1992: Predicting Atlantic seasonal hurricane activity 6-11 months in advance. *Weather Forecasting*, **7**, 440-455.

Gray, W.M., C. W. Landsea, P. W. Mielke Jr., and K. B. Berry, 1993: Predicting Atlantic basin seasonal tropical cyclone activity by 1 August. *Weather Forecasting*, **8**, 73-86

Gray, W.M., C. W. Landsea, P. W. Mielke Jr., and K. B. Berry, 1994: Predicting Atlantic basin seasonal tropical cyclone activity by 1 June. *Weather Forecasting*, **9**, 103-115.

Gray, W.M, 1998: Forecast probability of U.S. hurricane landfall for 1998. *Forecast Bulletin, published by the CSU team* http://typhoon.atmos.colostate.edu/forecasts/1998/prob98/index.html

Gray, W.M., C. W. Landsea, P. W. Mielke, K. J. Berry, 2000: Extended range forecast of Atlantic seasonal hurricane activity and US landfall strike probability for 2000. *Forecast Bulletin, published by the CSU team*

http://typhoon.atmos.colostate.edu/forecasts/2000/fcst2000

Helsel, D. R., R. M. Hirsch, 1992: Statistical methods in water resources. *Elsevier Science, Ltd.* 522pp.

Hess, J. C., and J. B. Elsner, and N. E. LaSeur, 1995: Improving seasonal predictions for the Atlantic basin. *Weather Forecasting*, **10**, 425-432.

Hurrell, J., 1995: Decadal trends in the North Atlantic Oscillation: regional temperatures and precipitation. *Science*, **269**, 676-679.

Kalnay, E., et al., 1996: The NCEP/NCAR 40-year reanalysis project, *Bulletin of American Meteorological Society* **77**, 437-471.

Neumann, C.J., Jarvinen, B.R., McAdie, C.J., and Elms, J.D. 1993: *Tropical Cyclones of the North Atlantic Ocean 1871-1992*. National Climate Data Center in cooperation with the National Hurricane Center, Coral Gables, FL, 193pp.

Pielke, Jr., R.A. 1997: Reframing the U.S. Hurricane Problem. *Society and Natural Resources*, **10**, 485-499.

Pielke, Jr. R. A., and Landsea, C. W. 1998: Normalized Atlantic hurricane damage, 1925 1995. *Weather and Forecasting*, **13**, 621-631.

Shapiro, L.J. 1982: Hurricane Climate Fluctuations. Part II: Relation to Large-Scale Circulation. *Monthly Weather Review*, **110**, 1014-1023.

Shapiro, L.J. 1989: The Relationship of the Quasi-biennial Oscillation to Atlantic Tropical Storm Activity. *Monthly Weather Review*, **117**, 1545-1552.

Shapiro, L.J. and Goldenberg, S.B. 1998: Atlantic Sea Surface Temperatures and Tropical Cyclone Formation. *Journal of Climate*, **11**, 578-590.

**Dr. Balaji Rajagopalan is currently an assistant professor at the Civil Engineering, Department at the University of Colorado in Boulder. Dr. Rajagopalan's research is focused on understanding the inter-annual variability of Atlantic Tropical Cyclone frequency and stochastic modeling of cyclone tracks, inter-annual variability of regional hydrology, and understanding the temporal variability of the Indian summer monsoon. He holds a Master of Science degree in operations research from Indian Statistical Institute, Calcutta, India and a Ph.D. in stochastic hydro-climatology and water resource from Utah State University.*

Email. Rajagopalan.Balaji@Colorado.edu

Dr. Yochanan Kushnir is a senior research scientist at Columbia University's Lamont-Doehrty Earth Observatory. His general research interest is climate data analysis with an emphasis on atmosphere-ocean interaction. He has

special interest in the study of the origin and impact of climate variability in and around the Atlantic Ocean Basin, including the phenomenon of the North Atlantic Oscillation and the climate of the tropical Atlantic. He lectures on topics of climate and its variability at Columbia University and the Weizmann Institute, Israel. He holds a Ph.D. in atmospheric sciences from Oregon State University.

Dr. Upmanu Lall is a Senior Research Scientist at the International Research Institute for Climate Prediction (IRI). Prior to joining the IRI, he was a professor at the University of Utah and Utah State University. He has over 20 years of experience as a hydrologist. Dr. Lall's principal areas of expertise are statistical and numerical modeling of hydrologic climatic systems and water resource systems planning and management. He *received his Ph.D. from the University of Texas in 1981.*

Jennie Miller has been a Staff associate with the Climate group at LDEO since 1998.

Arctic Oscillation and the East Asian Climate

By Daoyi Gong

Introduction

Many surface climate anomalies are directly brought on by fluctuations in the atmospheric circulation. Variability in temperature and precipitation on the local and regional scales are closely related to the atmospheric condition in the region of the target area as well as the global scale atmospheric variations. A number of studies have shown that the Arctic Oscillation (AO) is strongly coupled to surface air temperature fluctuations over the Eurasian continent.[1] AO's influence on the global and regional climate changes is currently the subject of much interest (Thompson and Wallace, 2001; Kerr 1999). The focus of this study is to investigate the AO's influence on variations of the climate over the eastern Asian region.

AO and the surface climate changes on the inter-annual time scale

The correlation coefficients between the AO index and temperatures over China are computated for wintertime (January-February-March: JFM) for 1958/59 and 1998/99. These results indicate that a positive relationship exists everywhere in China, except in the small regions over the southwestern Tibetan Plateau where the correlation coefficients vary from 0 to -0.2. The most significant areas cover the northern territory of China, north of 30°N-40°N, namely the northwestern, the northeastern, and the coastal regions (Figure 1). In these regions the correlation coefficients are above 0.3. This means that 16%~36% of the variance is associated with the AO. Thompson and Wallace (1998, 2000) have regressed northern hemispheric surface air temperature anomalies onto the standardized AO for JFM. They found that the positive phase of the winter AO is associated with positive surface air temperature anomalies throughout high latitudes of Eurasia. Regression coefficients vary from about 0.25 to 0.5 per standard deviation of the AO index over northern China. The results presented here are generally consistent with the previous findings but reveal more regional details.

The correlation coefficients between the AO index and precipitation are also calculated for the same period. It is interesting to note that the positive phase of the AO is generally associated with the positive precipitation anomalies, except for the small region in the northwest. The most significant relationship arises from two regions with values varying between 0.3 and 0.4. The larger area covers the central region of China between 30° to 40°N (east of 100°E) and a small area in the southern region of China close to the South China Sea. This means that about 10%-15% of the winter precipitation variance can be explained by the AO. The averaged precipitation over the entire inland

[1] Thompson and Wallace (1998) pointed out that the leading empirical orthogonal function of the wintertime northern hemisphere pressure field resembles the North Atlantic Oscillation but with more zonally symmetric appearance. This annular-like mode in the northern extratropical circulation is called Arctic Oscillation (AO). The AO has an equivalent barotropic structure from the surface to the lower stratosphere. Fluctuations in the AO create a seesaw pattern in which atmospheric pressure at the northern polar and middle latitudes alternates between positive and negative phase.

Figure 1. Time series of AO and the mean surface air temperature of 160-station in China during wintertime. To facilitate comparison all series are standardized regarding to 1961-90. The two curves correlate at 0.49, significant at 95% confidence level.

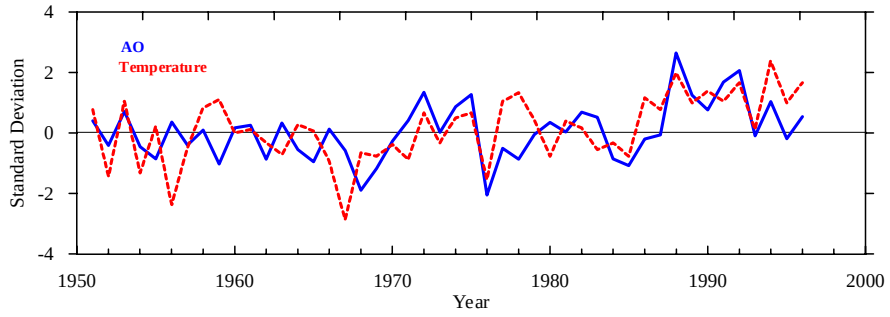

China also correlates with the AO at 0.47, this value is above the 95% confidence level.

Long-term climate variations

In this section the long-term variations of the AO and its connections to climate in China are analyzed by employing low-pass filtering techniques. Figure 2 shows the long-term time series of winter precipitation and temperature in China. Precipitation is computed from the mean of 33 stations over eastern China. All stations are located east of 100°E (Wang et al., 2000). This 33-station-mean series correlates to the 160-station-mean at 0.99 for the period 1951-1999. Temperature is the mean of Shanghai and Beijing. There is good spatial consistency in the temperature changes over China in winter as revealed by the empirical orthogonal function analysis (Wang et al., 1999), thus several typical stations may be enough for analysis. Here we chose only Beijing and Shanghai, this 2-station-mean series correlates to the 160-station-mean at 0.92 for the period 1951-1998.

A number of studies have demonstrated that there are interdecadal climatic variations in China. In order to compare the correlation between the climate and atmospheric indices on the interdecadal scale, a 10-40yr band-pass filter is applied to these long-term time series. The filtered low frequency components for these series are shown in Figure 2. To facilitate comparison, all series are normalized before filtering. Only the period from 1899 to1994 is shown here, due to the limit of data availability. In the above analysis it is found that there are good relationships between the AO, precipitation and temperature. As shown in Figure 2, these relationships are still evident, the correlation coefficients suggest that the AO plays a more significant role in both temperature and precipitation on the interdecadal time scale than on interannual time scale. The correlation between the AO and temperature is 0.68, for precipitation the correlation is even higher with a value of 0.72.

AO and the East Asian monsoon

Plenty of scientific evidence has indicated that the most important regional factor affecting winter climate in China is the Siberian High. An intensified Siberian High leads to a strong East Asian winter monsoon, which would give rise to a dramatic temperature changes over eastern Asia. Gong et al. (2001) reported that there is a significant out-of-phase relationship between the AO and Siberian High intensity. The Siberian High intensity is measured as the mean sea level pressure over the central region of the anticyclone. The correlation coefficient between these two indices is –0.48 for December-January-February (DJF) for the period 1958-98. It was found that the negative phase of the AO is concurrent with a stronger East Asian Trough and an anomalous anticyclonic flow over the Urals at the middle troposphere (500hPa). This anomalous circulation pattern could bring stronger northwesterlies and may enhance the upper-level airflow convergence in the rear of the trough. That means a weaker AO can be helpful to dynamically strengthen the Siberian High and winter monsoon, and vice versa.

The AO's influence on the East Asian winter monsoon and surface climate is evident over most of the continental Asia. Mean temperature averaged over middle to high latitude Asia (30°E-140°E, 30°N-70°N) is correlated to the Siberian High central intensity with correlation coefficient of -0.58 (1922-1999), and for precipitation, the correlation

Figure 2. Low frequent variations of AO (in black), temperature (in red) and precipitation (in blue). Shown as the results from a 10-40yr band-pass filter.

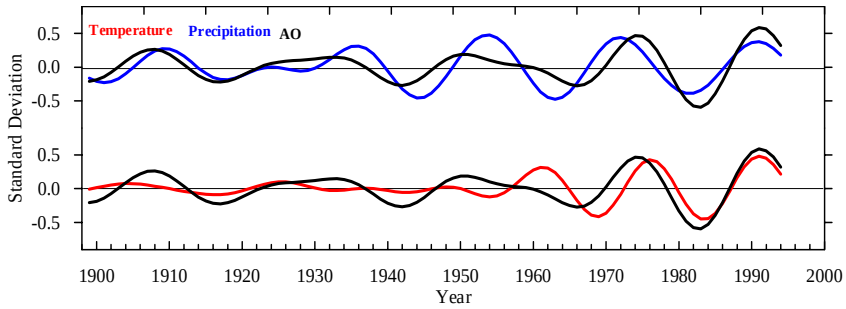

Table 1. Summary of correlation statistics for winter (JFM). * Significant at 95% confidence level. Shown in parentheses are sample numbers used to compute the correlation. The sample numbers are variable due to the data availability. Precipitation and temperature are means for continental Asia averaged over middle to high latitude Asia (30°E-140°E, 30°N-70°N).

	AO	EU	SO	Precipitation	Temperature
Siberian High	-0.52*(76)	0.30*(52)	0.14(79)	-0.44*(77)	-0.58*(78)
AO	1	-0.37*(49)	0.12(76)	0.14(76)	0.53*(76)
EU		1	-0.07(52)	-0.28*(50)	0.21(51)
SO			1	-0.38*(77)	-0.28*(78)

coefficient is -0.44 (1922-1998). Of course, some other circulation systems such as Southern Oscillation Index (SOI) and Eurasian teleconnection pattern (EU) are also found to be responsible for the climatic changes over mid to high latitudes to some extent (Hurrell, 1996, Zhu et al, 1997). Co-variability values among some components are listed in Table 1. To check the contribution by these elements, a multiple regression analysis is applied to these indices. For the sake of establishing equal record length among the indices, all data are adjusted to the period from 1949 to 1997. The Siberian High, AO, EU and SO all together can explain 72 percent of the variance in temperature. The isolated variance reveals that the AO-related change is the most important, with a contribution of 30%. The Siberian High explains 24% of the variance in temperature. The fractions related to EU and SO are 11% and 7%, respectively. The precipitation variance explained by the AO and Siberian High is relatively low, both less than 10%.

Given the evidence of strong influence of winter-half-year AO on the surface conditions (snow, temperature, sea-ice, sea surface temperature, etc.), one can propose that the AO may not impact only the wintertime climate, but also the summer condition. A recent study shows that the AO also exerts significant influences on year-to-year variations in the East Asian summer monsoon rainfall (Gong and Ho, 2002). The correlation between late spring AO and precipitation shows well-defined features over East Asia (Figure 3). Mean summer precipitation averaged over ten stations located at southern Japan and middle China (along the famous *Meiyu-Baiu* rainfall belt) is used to measure the summer monsoon rainfall. When the AO leads by one month, the correlation between the May-July AO and summer monsoon rainfall is -0.44. When AO leads by two months, the correlation becomes -0.32. The May AO index shows the strongest connection to the summer monsoon rainfall, with correlation coefficient of -0.45. Large-scale atmospheric circulation patterns in East Asia in association with the AO are also evident. A positive phase of the AO

Figure 3. Changes in summer precipitation (mm) corresponding to a one standard deviation of the May AO index for the period 1900-1998. Regions above 95% confidence level are shaded. The contour interval is 10 mm. Zero contours are omitted. Filled circles are ten stations with data available for the entire period of 1899-

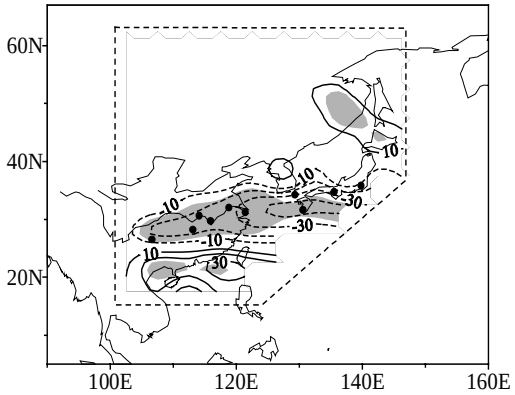

in late spring is found to lead to a northward shift in the summertime upper tropospheric jet stream over East Asia. This northward shift of the jet stream is closely related to an anomalous sinking motion in 20º-40ºN and a rising motion in surrounding regions. These changes give rise to drier conditions over the region extending from the Yangtze River valley to southern Japan and wetter conditions in southern China. Possible mechanisms connecting the late spring AO and summer monsoon rainfall remain to be addressed.

Conclusion

AO has a strong influence on the climate in East Asia. During the high-AO years, warmer than normal temperature and precipitation are observed over most of China in winter. On the interdecadal time scale, the AO also shows significant influences on both temperature and precipitation.

It is also revealed that the AO significantly impacts the East Asian winter monsoon through the Siberian High. A weak AO gives rise to the strong Siberian High and winter monsoon. Evidence also shows that there are significant connections between the late spring AO and East Asian summer monsoon and monsoon rainfall; a positive-strong-AO usually leads to less summer monsoon rainfall along the Yangtze River and southern Japan.

Suggested references and web sites

- For more information on AO and its definition see:

Thompson, D. W. J., and J. M. Wallace, 1998: The Arctic Oscillation signature in the wintertime geopotential height and temperature fields, *Geophysical Research Lett*ers, **25**, 1297-1300.

- For more information on AO's climatic influence see:

Gong, D.Y., S.W. Wang, and J.H. Zhu, 2001: East Asian winter monsoon and Arctic Oscillation. *Geophysical Research Letters*, **28**(10), 2073-2076.

Gong, D. Y., and C. H. Ho. Arctic Oscillation Signals in the East Asian Summer Monsoon, 2002: *Journal Geophysical Research - Atmosphere*, in press.

Kerr R. A., 1999: A new force in high-latitude climate. *Science*, **284**,241-242.

Thompson, D. W. J., and J. M. Wallace, Annular modes in the extratropical circulation, Part I: Month-to-month variability. *Journal of Climate*, **13**(5), 1000-1016.

Thompson, D. W. J., and J. M. Wallace, Regional climate impacts of the Northern Hemisphere annular mode. *Science*, **293**,85-89.

Thompson, D. W. J., J. M. Wallace, and C. Gabriele, Annular modes in the extratropical circulation, Part II: Trends. *Journal of Climate*, **13**(5), 1018-1036.

- Information on AO can also be obtained at:

http://nsidc.org/arcticmet/patterns/arctic_oscillation.html

http://tao.atmos.washington.edu/wallace/ncar_notes/

Dr. Daoyi Gong is an associate Professor at the Key Laboratory of Environmental Change and Natural Disaster, Beijing Normal University, China. Dr. Gong's research is focused on the variability of the atmospheric oscillations and the historical climate change in Asia. He holds a master's degree in physical Geography from Beijing Normal University, and a Ph.D. in Climatology from Beijing University.

Email. gdy@pku.edu.cn

Upcoming Events

NOAA 27th Annual Climate Diagnostics and Prediction Workshop
October 21-25, 2002
Fairfax, Virginia
http://www.cpc.noaa.gov

Climate Prediction Assessments Workshop: Research and Applications on Use and Impacts
October 28-30, 2002
Washington, DC
http://www.ogp.noaa.gov/

83rd Annual conference of the American Meteorological Society
February 9-13, 2003
Long Beach, CA
http://www.ametsoc.org/

The Climate Report
Volume 3, Number 3
Summer 2002

Publisher
The Climate Report is a quarterly publication of Climate Risk Solutions, Inc.
233 Harvard Street, Suite 307
Brookline, MA 02446 U.S.

Editor Maryam Golnaraghi

Contributing Editor
A Hossein Farman-Farmaian

Production Intoto, Inc.

Subscriptions
Tel: 617.566.0077
Fax: 617.566.2750
E-mail: info@climaterisksolutions.com